J. Chem. Soc., Faraday Trans. 2, 1989, **85**(8), 1325–1335

Rotational Alignment of NO from Pt(111)

Inelastic Scattering and Molecular Desorption

Dennis C. Jacobs,*† Kurt W. Kolasinski, Robert J. Madix and Richard N. Zare

Department of Chemistry, Stanford University, Stanford, California 94305, U.S.A.

The rotational alignment distribution of NO has been measured subsequent to the molecule's interaction with a well characterized Pt(111) surface. Internal state distributions have been probed using 1 + 1 resonance-enhanced multiphoton ionization (REMPI) spectroscopy in which lines of the NO $A\,^2\Sigma^+$–$X\,^2\Pi$ (0, 0) band constitute the resonant transition. NO/Pt(111) scattering has been studied in two distinct regimes: inelastic scattering and trapping/desorption. In both cases, there is relatively no preferential alignment of rotation for $J < 12.5$. However, molecules with higher rotational angular momentum show a marked increase in alignment. Inelastically scattered molecules prefer to rotate in a plane normal to the surface ('cartwheel' motion), whereas desorbing molecules prefer to rotate in a plane parallel to the surface ('helicopter' motion). These measurements provide new insight into momentum transfer at surfaces and the nature of the transition state which leads to molecular desorption.

Rotational dynamics at the gas–surface interface reveal unique information about the molecule–surface potential. A molecule passing from the constrained two-dimensional environment of a solid surface lattice into a three-dimensional vacuum has the potential for exhibiting strong rotational polarization.

Here, we investigate the rotational alignment of NO after it interacts with a Pt(111) surface. We examine experimentally two distinct dynamical regimes, inelastic scattering and trapping/desorption. The first refers to a collision of short duration (one or a few bounces) between the molecule and the surface. This scattering event leaves the molecule with an energy distribution characteristic of both the molecule's initial conditions and the nature of the surface. The second involves a relatively long surface residence time in which the molecule completely loses 'memory' of its initial conditions. In this latter case, the desorbed molecule's energy distribution is characterized solely by the conditions of the surface and the molecule–surface potential.

There have been only two prior studies in which rotational alignment has been measured for gas–surface scattering: NO/Ag(111)[1-3] and N_2/Ag(111).[4-6] These experiments both probed the regime of direct inelastic scattering by impinging an energetic supersonic molecular beam (10–90 kJ mol^{-1}) on a relatively cold Ag(111) surface. Kleyn and co-workers[1-3] measured a preference for NO to scatter from Ag(111) with its rotational motion resembling that of a 'cartwheel' (fig. 1). This behaviour is reconciled with a simple hard-cube model which permits forces only along the surface normal. These forces deliver an anisotropic torque on the molecule, causing an observed preference for cartwheel motion. Zare and co-workers[4-6] found a similar result for N_2/Ag(111). Additionally, they measured the rotational orientation resulting from surface scattering. They observed a strong correlation between rotational orientation, rotational quantum number and scattering exit angle.

Electric-field deflection techniques have probed surface scattering dynamics through the observation/preparation of molecular orientation. Novakoski and McClelland[7]

† Present address: Department of Chemistry, University of Notre Dame, Notre Dame, IN 46556, U.S.A.

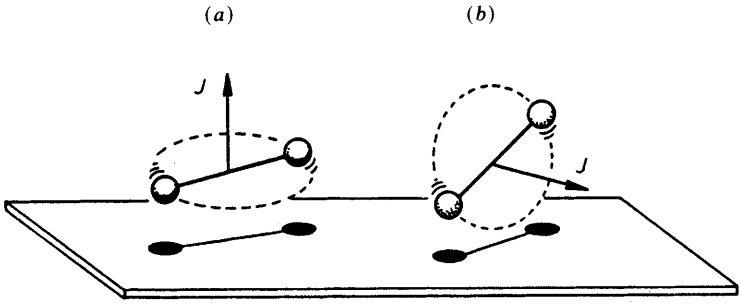

Fig. 1. Rotational alignment relative to the surface plane. The helicopter motion (*a*) is preferred for $A_0^{(2)} > 0$; the cartwheel motion (*b*) is favoured for $A_0^{(2)} < 0$.

measured a preferential molecular orientation for the desorption of CHF_3 from Ag(111), *i.e.* CHF_3 tends to desorb with its hydrogen atom orientated toward the surface. Additionally, they found that scattering leaves the molecule with a weak orientation in the opposite sense. More recently, Kuipers *et al.*[8] observed the scattering angular distribution of NO from Ag(111), where the incident NO was orientated in predominantly two opposite directions relative to the surface. There appeared to be a greater loss in normal translational energy when the oxygen atom, rather than the nitrogen atom, was directed toward the surface.

The present study represents the first observation of rotational alignment in desorption. Additionally, it reports the rotational alignment of scattered NO in a previously unexplored regime, one in which the molecule's final rotational energy exceeds the initial energy of the incident molecular beam. Here, surface vibration–rotational energy transfer is the operative mechanism. The experiment utilizes 1+1 REMPI through the NO A $^2\Sigma^+$–X $^2\Pi$ (0, 0) band to measure rotational alignment distributions in a state-specific manner. The quantitative reduction of 1+1 REMPI spectra to alignment moments requires inclusion of both saturation in the resonant transition as well as incorporation of the symmetry character of the ionization transition. We present a brief summary of the methodology employed for the extraction of the quadrupole moment of the rotational alignment distribution from 1+1 REMPI spectral intensities.

Experimental

The experiment utilizes an ultra-high vacuum (u.h.v.) scattering chamber, a tunable u.v. laser source and a variety of support electronics, all of which are described in detail elsewhere.[9] A schematic diagram of the apparatus is shown in fig. 2. In short, the u.h.v. chamber is equipped with a sample manipulator (to facilitate sample translation rotation, surface heating and cooling), LEED and Auger surface diagnostics (to monitor surface order and cleanliness), a pulsed molecular beam source, a port for entry of a laser beam and ion time-of-flight tube. The main chamber is pumped by a 220 $dm^3\,s^{-1}$ ion pump, a titanium sublimation pump, a liquid-nitrogen cryopanel and a 1500 $dm^3\,s^{-1}$ turbo-molecular pump (base pressure 2×10^{-10} Torr†).

A differentially pumped invaginated source chamber houses the pulsed valve/skimmer assembly. The supersonic beam (50 psi‡ neat expansion through a 0.1 mm nozzle orifice) is collimated with a 0.3 mm skimmer so that the beam strikes only a 5 mm

† 1 Torr = 101 325/760 Pa.
‡ 1 psi = $6.894\,76\times10^3$ Pa.

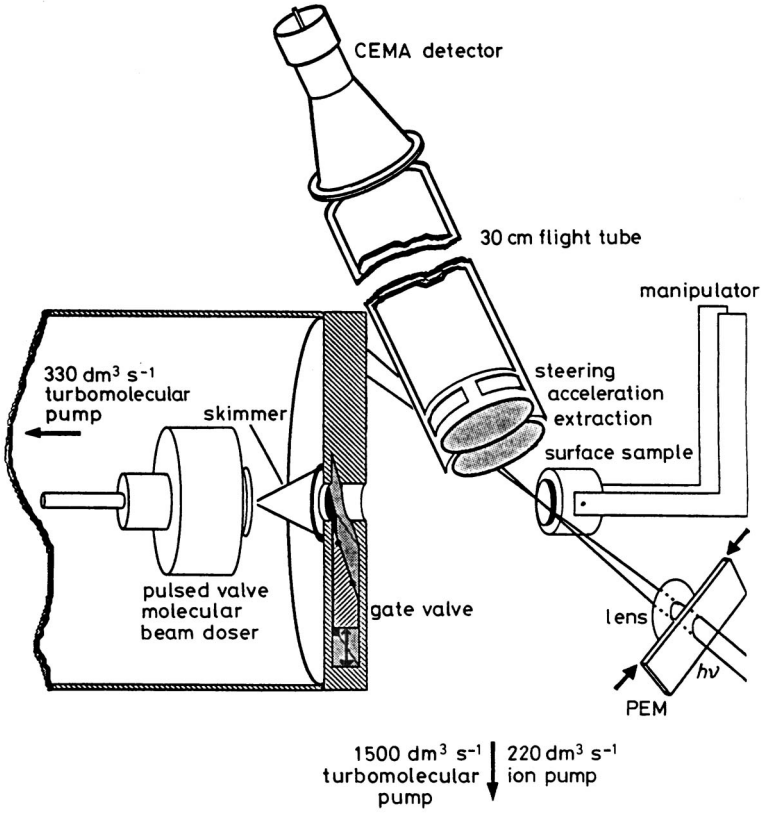

Fig. 2. Experimental apparatus. A differentially pumped pulsed valve doses the Pt(111) crystal. Laser radiation is focussed 2 mm above the surface. Ions produced in the REMPI process are accelerated through the time-of-flight tube and collected by the CEMA charged particle multiplier. The crystal can be rotated in order to face LEED and Auger diagnostics. Not shown are Helmholtz coils which cancel the earth's magnetic field and leave a residual magnetic field in the direction of the surface normal.

diameter region of the surface. The 10 cm nozzle–surface distance allows instantaneous pulsed molecular beam fluxes as high as 10^{17} molecule $cm^{-2}\,s^{-1}$. The rotational temperature of the neat beam is measured at 40 K and the beam translational energy is estimated to be 9 kJ mol^{-1}.[10] A 330 $dm^3\,s^{-1}$ turbomomecular pump establishes a base pressure of 1×10^{-8} Torr in the source chamber.

The generation of tunable ultraviolet laser radiation relies on a commercial 10 Hz Quantel Nd:YAG system. The output of the dye laser (0.08 cm^{-1} bandwidth) is frequency-doubled and Raman shifted (second-order anti-Stokes) in H_2. This system creates 6 ns pulses at 224 nm with *ca.* 200 μJ per pulse. A portion of the resulting laser beam is loosely focussed into the chamber (10 mJ cm^{-2} fluence). The direction of linear polarization is selected, on a shot-to-shot basis, by a photoelastic modulator (PEM) interfaced to a DEC PDP 11/23 computer. The energy of each laser pulse is measured by a pyroelectric detector and stored in the computer.

The laser light runs parallel to and passes 2 mm above the surface. A fraction of the molecules leaving the surface pass through the laser interaction region and become ionized by the laser radiation *via* the REMPI process. The resulting ions are accelerated through a time-of-flight tube and collected by a charged particle multiplier (CEMA

multichannel plates). The ion signal is digitized by a CAMAC charge-sensitive gated integrator and passed to the computer for storage.

Owing to the $^2\Pi$ symmetry of the NO ground state, stray magnetic fields can scramble the rotational alignment of the product distribution during the molecule's 1 μs flight time from the surface to the laser ionization region. In order to minimize stray magnetic fields,[11] Helmholtz coils are installed around the exterior of the main chamber. The regulated currents flowing through these coils are adjusted so that a small field, pointing along the surface normal, remains in the ionization region.† In addition, the filament current used to heat the surface is turned off for 10 ms during the laser pulse.

The dynamical regimes of direct inelastic scattering and trapping/desorption are differentiated according to their characteristic surface residence times. The residence time for direct inelastic scattering is infinitesimal on the microsecond timescale of the molecular-beam pulse. However, the trapped state will exhibit a half-life on the surface which is inversely proportional to the desorption rate constant. For our temperature regime, the half-life is estimated to be 2–2000 ms. Synchronizing the laser to fire during the nozzle pulse discriminates in favour of those molecules which have inelastically scattered. Conversely, firing the laser 200 μs after the 90 μs nozzle pulse precludes inelastic scattering contributions and permits only detection of those molecules which have trapped and subsequently desorbed. The surface coverage at which these experiments are performed is less than 3% of a monolayer.

Analysis

The accurate analysis of 1+1 REMPI spectra of NO through the $A\,^2\Sigma^+$–$X\,^2\Pi$ (0, 0) band requires characterization of both the extent of saturation in the resonant step as well as the M_J-dependence of the ionization step. There are two stages in which the 1+1 REMPI data are treated. First, the data are power-normalized to account for variations in the laser power arising from shot-to-shot fluctuations and changes in the laser gain across the dye curve. In real time, the computer corrects the ion signal for variations in the laser energy through a least-squares fitting routine described elsewhere.[12] Secondly, the normalized data are reduced to population and alignment distributions while considering saturation of the resonant step and variations in the ionization probability with M_J (the projection of $\boldsymbol{J}$ on the laser polarization direction).[12]

Our findings indicate that for our required sensitivity range, partial saturation is unavoidable. Complete saturation, however, eliminates all chances of measuring rotational alignment. Therefore we choose to work in a regime of moderately weak saturation and take great care in the reduction of population and alignment moments to remove the detrimental effects of saturation.

The second photon absorbed in a 1+1 REMPI scheme excites a continuum transition in the molecule. The dipole moment of ths transition points in some direction relative to the internuclear axis. The limiting direction of the transition dipole moment is either parallel or perpendicular to the internuclear axis. The projection of the dipole transition moment onto the internuclear axis directly determines the M_J-dependent transition probability for the ionization step. This is required because different branch excitations in the resonant step create different alignment distributions in the intermediate level. The probability for ionization from the intermediate level is a function of both the intermediate-state alignment created by resonant excitation and the fraction of parallel *versus* perpendicular character in the ionization transition.

Fortunately, rotational populations extracted from different branch excitations reveal redundant information. Additionally, different branches saturate at different laser power

† A magnetic field along the cylindrical symmetry axis will not affect the observed alignment. Instead, it will ensure that stray transient fields will be insufficient to alter the net field direction.

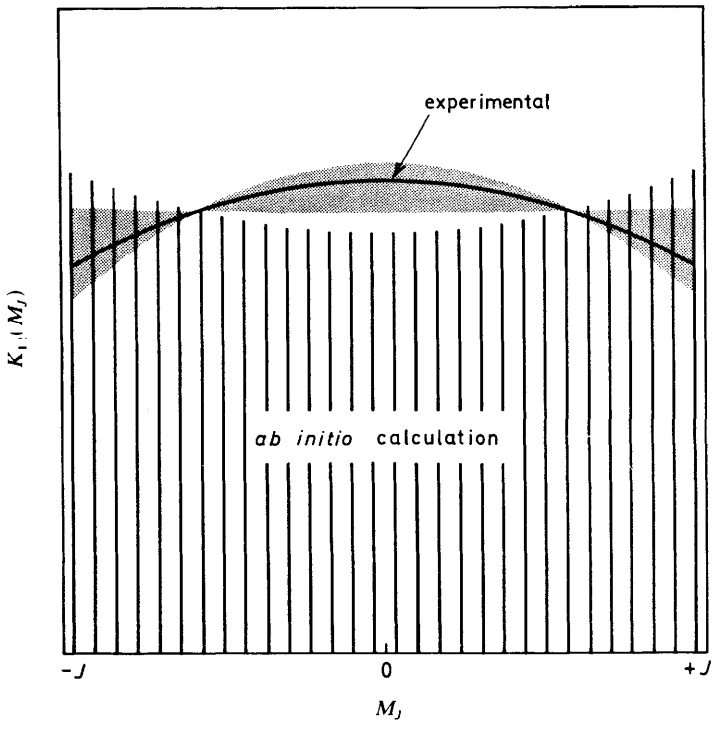

Fig. 3. The M_J-dependence of the ionization step in 1 + 1 REMPI of NO through the $A\,^2\Sigma^+$-$X\,^2\Pi$ (0, 0) band. The solid curve and shaded region represent the best fit and corresponding uncertainty in the experimental measurement.[12] The vertical lines are calculated theoretically by *ab initio* methods.[21]

levels because of variations in the rotational line strength with branch excitation. Calibration spectra of NO in a room-temperature bulb are utilized to determine both the extent of saturation and the M_J-dependent ionization probability in the 1 + 1 REMPI process. This information is then used to analyse nascent distributions arising from NO molecules which have been scattered and desorbed from the Pt(111) surface.

The experimentally measured M_J-dependent ionization probability is shown in fig. 3,[12] which reveals a relatively slight variation in the ionization transition probability with the quantum number, M_J. This has the consequence of limiting the amount of rotational alignment information which can be extracted from 1 + 1 REMPI of NO. Rotational alignment is conveniently described by the even moments of the rotational angular distribution. In the case of cylindrical symmetry, 1 + 1 REMPI through the NO A-X(0, 0) band will only be sensitive to the population and the quadrupole moment, $A_0^{(2)}$.[11,12] Because of the ionization dynamics, the $A_0^{(4)}$ moment cannot be extracted with any sensitivity. The value of the quadrupole moment ranges from +2 to −1,[13] where these limits correspond to the molecule rotating in a plane parallel to the surface ('helicopter' motion) or in a plane perpendicular to the surface ('cartwheel' motion), respectively (see fig. 1). A quadrupole moment of zero suggests no preferential alignment of rotation, *i.e.*, an isotropic distribution.

Extraction of the population and quadrupole alignment moments requires that the ion signal be recorded for only two independent planes of linearly polarized light. In the laboratory, we record spectra under conditions where the polarization direction of the laser is either parallel or perpendicular to the surface normal. This is performed by

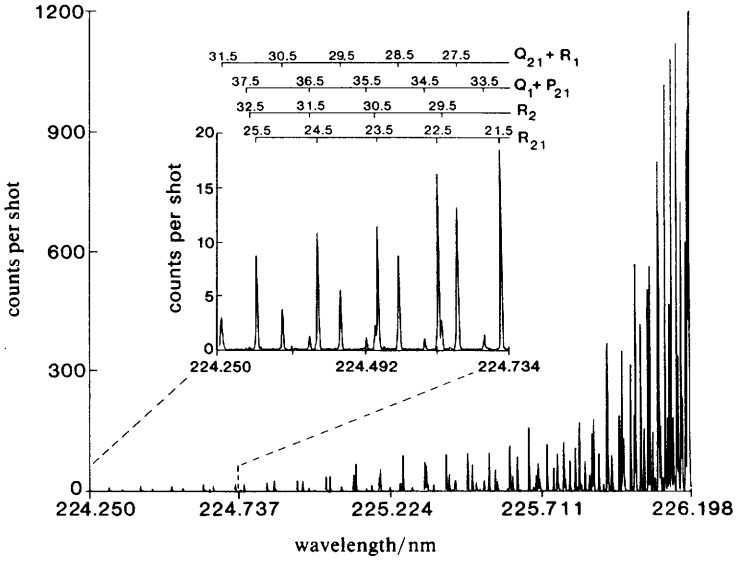

Fig. 4. Spectrum of NO scattering from a Pt(111) surface at 400 K. The inset provides an expanded view of the high-J region. The rotational transitions of the resonant excitation step are assigned.

alternating the polarization between these two directions throughout an entire wavelength scan. For a given rotational transition out of a rotational state J, we identify $I_{\parallel}$ and $I_{\perp}$ as the integrated ion intensities for which the laser polarization was parallel or perpendicular to the surface normal (the cylindrical symmetry axis), respectively. The quadrupole alignment moment $A_0^{(2)}(J)$ is related to these measured intensities by

$$A_0^{(2)}(J) = \frac{2\{I_{\parallel} - I_{\perp}\} \sum_{M_J} F_{\mathrm{sat}}[k_{01}(M_J), k_{12}(M_J), I\Delta t]}{\{I_{\parallel} + 2I_{\perp}\} \sum_{M_J} \left(3\frac{M_J^2}{J(J+1)} - 1\right) F_{\mathrm{sat}}[k_{01}(M_J), k_{12}(M_J), I\Delta t]} \quad (1)$$

where M_J is the quantum number representing the projection of $\boldsymbol{J}$ on the cylindrical symmetry axis, $k_{01}(M_J)$ is the M_J-dependent transition probability for the resonant photon step, $k_{12}(M_J)$ is the M_J-dependent transition probability for the ionization step, $I\Delta t$ is the measured laser fluence and F_{sat} is a function which calculates the overall 1+1 REMPI ionization probability while including the effects of saturation and intermediate-state alignment. The analytical form of F_{sat}, as well as $k_{01}(M_J)$ and $k_{12}(M_J)$, have been worked out previously.[11,12]

Results

Inelastic Scattering

The dynamical regime of inelastic scattering is selectively explored by firing the laser synchronously with the rising edge of the nozzle gas pulse.† A typical spectrum of NO scattered at normal incidence from a 400 K Pt(111) surface is shown in fig. 4. This

† Normal incidence/normal detection prohibits angular discrimination against the incident molecular beam. Temporal discrimination is also impossible because of the slow falling edge on the molecular-beam pulse relative to the flight time of the molecules (0.5 mm μs^{-1}). However, owing to the low rotational temperature of the beam, interference from the beam will affect only the states $J < 7.5$.

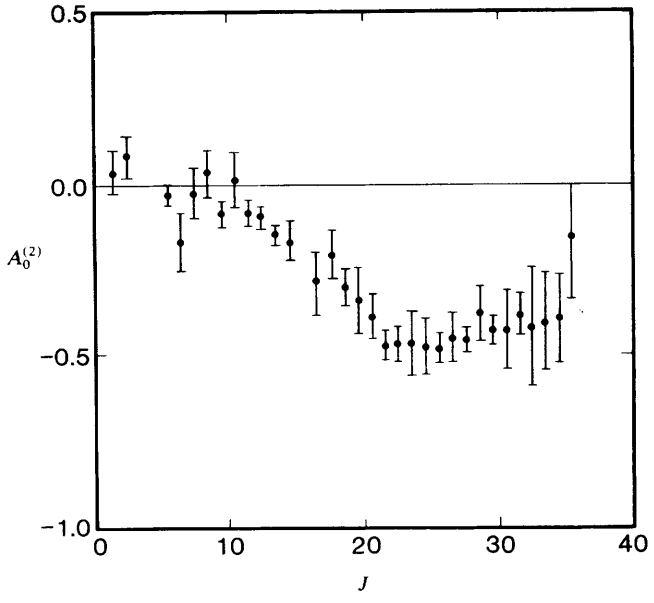

Fig. 5. Quadrupole moment alignment distribution as a function of the rotational quantum number J plotted for the case of inelastic scattering of NO from Pt(111) at 400 K.

portion of the spectrum contains predominantly branches originating from the $^2\Pi_{1/2}$ ground spin–orbit state. A section of the figure is expanded to illustrate the high signal-to-background ratio that is routinely realized with 1+1 REMPI.

The spectra, recorded at orthogonal laser polarizations, are reduced to population and alignment distributions. The population distributions show considerable rotational excitation and are reported elsewhere.[9] Fig. 5 shows the quadrupole alignment moment for the scattered molecules *versus* their rotational quantum number J. For $J < 12.5$ there is no appreciable alignment. Of course, interference by the incident beam will dilute the amount of observable alignment in this region. Beyond $J = 12.5$ there is a steady rise in the rotational alignment until it peaks near $J = 25.5$. The maximum alignment observed corresponds to a quadrupole moment of -0.5. Recall that $A_0^{(2)}$ has a limiting value of -1, which occurs when all the molecules rotate with a cartwheel-type motion. For $J > 25.5$, the alignment appears to decrease slightly.

For clarity, fig. 5 includes only the quadrupole moment values measured for the $^2\Pi_{1/2}(A'')$ state. Here, the A″ notation refers to the symmetry of the ground-state Λ-doublet.[14] Measurement of the rotational alignment in the A′ state of the $^2\Pi_{1/2}$ level is difficult because of congestion in one branch and branch-mixing in the other. However, the two Λ-doublets of opposite symmetry in the $^2\Pi_{3/2}$ state exhibit similar rotational alignment distributions.

Trapping/Desorption

The desorption regime is isolated by firing the laser 200 μs after the completion of the nozzle pulse,† thus eliminating contributions from inelastic scattering channels. The Pt(111) sample is held at 553 K, while the molecular beam delivers pulses of NO to the

† The nozzle pulse is characterized by a fast rising edge and a relatively slow tailing edge. Care is taken to ensure that the laser fires well after the visible tail of the pulse.

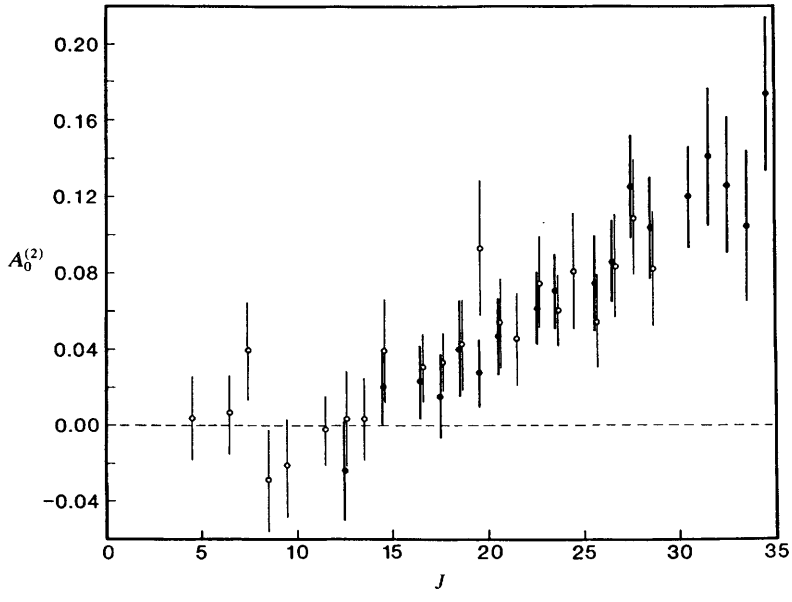

Fig. 6. Quadrupole moment alignment distribution for NO desorption plotted against rotational quantum number *J*. The Pt(111) surface temperature is 553 K. ○, R_{21} branch member; ●, $Q_1 + P_{21}$ branch member.

surface at 10 Hz. Because of the low signal intensity in this operating regime, accurate alignment moments cannot be extracted during the course of a wavelength scan. Therefore, the laser is tuned to a specific rotational transition and ions are collected for 1000–10 000 laser shots at alternating laser polarization directions. The measured intensities are analysed using eqn (1).

Fig. 6 shows the quadrupole moment, $A_0^{(2)}(J)$, as calculated from two different rotational branches of the same $^2\Pi_{1/2}$ Λ-doublet state.[15] There is little to no rotational alignment for $J < 12.5$, while higher rotational levels show increasing values of the quadrupole moment. A positive quadrupole moment indicates a preference for rotational motion similar to that of a helicopter (see fig. 1). As in the case of direct inelastic scattering, the Λ-doublet states in both spin–orbit levels exhibit similar degrees of alignment.

Discussion

The technique of 1+1 REMPI spectroscopy successfully probed rotational alignment in NO, subsequent to its interaction with a Pt(111) surface. The extraction of alignment information from 1+1 REMPI spectra requires a methodology which incorporates the effects of saturation in the resonant step and intermediate state alignment in the ionization step. As a check, the quadrupole moment was reduced from the polarization dependence of both R_{21} and $Q_1 + P_{21}$ branch members. While the polarization ratios of these two branches show opposite preferences, they reduce to the same values of the quadrupole moment for each rotational level *J*.

These experiments cover new ground in the field of gas–surface dynamics. They represent the first observation of rotational alignment in molecular desorption. Additionally, this marks the first study of inelastic scattering in which rotational levels up

to three times more energetic than the incident-beam energy are examined for rotational alignment. Although significant surface to rotational energy transfer is responsible for populating states with rotational energy exceeding the beam energy, rotational alignment is created in these states and is preserved in the final distribution. The observation of opposite preferences for rotational alignment in desorption and inelastic scattering further exemplifies the interesting dynamics at work in this chemical system.

Both inelastic scattering and trapping/desorption regimes yield little rotational alignment for the levels, $J < 12.5$, while higher rotational levels show a monotonic increase in the magnitude of the quadrupole moment. For the case of desorption the alignment distribution implies a preference for helicopter motion. In contrast, the inelastic scattering process produces an alignment distribution which is indicative of cartwheel motion. Although both types of gas-surface interactions involve the same molecule-surface potential, their dynamics differ because of the way the molecule enters and exits the potential well. The following interpretations are supported by classical trajectory calculations which were performed to simulate the dynamics of the NO/Pt(111) interaction.[16]

In the case of inelastic scattering, the quadrupole moment shows a similar preference toward cartwheel motion as that seen for the scattering of NO[1-3] and N_2[4-6] from Ag(111). The preference for cartwheel motion in inelastic scattering arises from the predominantly out-of-plane forces that the molecule experiences during the impulsive surface collision. These forces torque the molecule such that it rotates in a plane normal to the surface. For NO/Pt(111), the observed quadrupole moment peaks at a value of -0.5.

There are four possible reasons why the quadrupole moment might not reach its limiting value of -1. First, corrugation in the surface potential introduces tangential forces that are not present on a flat surface. Hence, on a corrugated surface the molecule can receive torques which induce rotational motion in a plane other than the pure cartwheel limit predicted for a flat surface. Secondly, multiple bounces on the surface will scramble alignment, as demonstrated by the trajectory model presented elsewhere.[16] This effect potentially differentiates direct inelastic scattering from indirect inelastic scattering. Thirdly, the low populations in the highest rotational levels are susceptible to a weak but non-negligible contribution from trapping/desorption. This contribution would most likely have the opposite sense of alignment (as seen in the desorption results reported here) and thus affect the observed alignment more dramatically. Fourthly, breaking cylindrical symmetry in the system introduces new non-vanishing moments to the measured alignment distribution. The consequence of this effect is that measurement is made of the 'apparent' quadrupole moment rather than the true quadrupole moment.[17] However, we believe that deviations from cylindrical symmetry are minimal for this system.

The quadrupole moment distribution measured for the case of molecular desorption is quite surprising. For rotational states with $J > 12.5$ a positive quadrupole moment is observed. The maximum measured quadrupole moment (+0.15) implies that 1.2–1.5† times as many molecules desorb with their plane of rotation resembling that of a helicopter as those resembling a cartwheel motion. The observed alignment cannot be reconciled with the simple picture of a direct transition from the known low-temperature equilibrium position (NO bound normal to the surface) to the gas-phase free rotor without the existence of an intermediate state occupied immediately prior to desorption. Our measurements are sensitive to the last few interactions the molecule makes with the surface before being desorbed, *i.e.* the nature of the molecule-surface potential near

† The limiting values of this range assume that the rotational alignment distribution is best described by either an ellipsoid or a function which contains a linear combination of $\cos^2\theta$ and $\sin^2\theta$, respectively. The trajectory calculations suggest that the latter function provides a more accurate description of the distribution. In any case, these two functional forms probably represent the limiting cases for the alignment distribution.

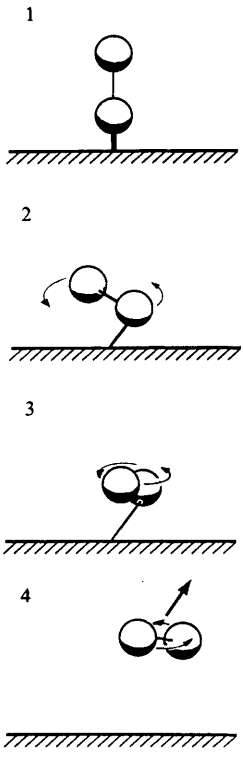

Fig. 7. Proposed mechanism for desorption. Frame 1 shows the low-temperature equilibrium geometry for NO on Pt(111). Rotation on the surface is less hindered in the plane parallel to the surface. Frames 2 and 3 show a rotationally excited species on the surface. Cleavage of the chemisorption bond (frame 4) leads to a preference for 'helicopter' motion in the escaping NO molecule.

the transition state. Rotation in the plane of the surface is less hindered than rotation in a plane normal to the surface because the former motion never forces the repulsive O end of the molecule closer to the surface than the attractive N end. This implies that there exists a higher density of rotational states associated with helicopter motion on the surface than those associated with a cartwheel motion. Thermal population of these surface hindered-rotor states[18] followed by cleavage of the molecule-surface bond will leave the desorbed molecule with a preference toward helicopter motion (fig. 7).

The observed rotational alignment distribution for molecular desorption is not inconsistent with the NO/Pt(111) measurements of Ertl and co-workers[19] and Mantell *et al.*[20] The first group measured no detectable change in the populations extracted from Q-branch excitations relative to those of P and R branches.[19] This is a relatively insensitive measure of rotational alignment and the magnitude of their error bars precludes a quantitative determination of the quadrupole moment. Additionally, the maximum rotational quantum state which they were able to observe was $J = 23.5$. The latter study of Mantell *et al.* imposed the following limit on the quadrupole moment: $A_0^{(2)}(J) < |0.1|$ for $J = 4.5$ and $J = 12.5$.[20] This agrees well with our reported value of $A_0^{(2)}(J) = 0.0 \pm 0.04$ for these two quantum levels. Additionally, the experiments of Mantell *et al.*[20] were performed at a much higher coverage and lower temperature than those reported here. At higher coverages, lateral interactions become important and these may inhibit rotational motion in the plane parallel to the surface.

In conclusion, the ability to make quantitative measurements of the polarization dependence of 1+ REMPI allows us to determine rotational alignment. Such rotational alignment measurements provide new insight into the highly anisotropic processes of inelastic scattering and trapping/desorption of molecules on surfaces.

This work was supported by the Office of Naval Research (N00014-87-K-00265). We gratefully acknowledge the assistance of Stacey F. Shane.

References

1 A. Luntz, A. Kleyn and D. Auerbach, *Phys. Rev. B*, 1982, **25**, 4273.
2 A. Kleyn, A. Luntz and D. Auerbach, *Surf. Sci.*, 1983, **117**, 33.
3 A. Kleyn, A. Luntz and D. Auerbach, *Surf. Sci.*, 1985, **152**, 99.
4 G. O. Sitz, A. C. Kummel and R. N. Zare, *J. Vac. Sci. Technol. A*, 1987, **5**, 513.
5 G. O. Sitz, A. C. Kummel and R. N. Zare, *J. Chem. Phys.*, 1987, **87**, 3247.
6 G. O. Sitz, A. C. Kummel and R. N. Zare, *J. Chem. Phys.*, 1988, **89**, 2558.
7 L. V. Novakoski and G. M. McClelland, *Phys. Rev. Lett.*, 1987, **59**, 1259.
8 E. W. Kuipers, M. G. Tenner, A. W. Kleyn and S. Stolte, *Nature* (*London*), 1988, **334**, 420.
9 D. C. Jacobs, K. W. Kolasinski, S. F. Shane and R. N. Zare, *J. Chem. Phys.*, submitted.
10 J. A. Serri, M. J. Cardillo and G. E. Becker, *J. Chem. Phys.*, 1982, **77**, 2175.
11 D. C. Jacobs and R. N. Zare, *J. Chem. Phys.*, 1986, **85**, 5457.
12 D. C. Jacobs, R. J. Madix and R. N. Zare, *J. Chem. Phys.*, 1986, **85**, 5469.
13 C. H. Greene and R. N. Zare, *J. Chem. Phys.*, 1983, **78**, 6741.
14 M. Alexander, P. Andreson, R. Bacis, R. Bersohn, F. Comes, P. Dagdigian, R. Dixon, R. Field, G. Flynn, K. Gerecke, E. Grant, B. Howard, J. Huber, D. King, J. Kinsey, K. Kleinermanns, K. Kuchitsu, A. Luntz, A. McCafferty, B. Pouilly, H. Reisler, S. Rosenwaks, E. Rothe, M. Shapiro, J. Simons, R. Vasudev, J. Wiesenfeld, C. Wittig and R. Zare, *J. Chem. Phys.*, 1988, **89**, 1749.
15 D. C. Jacobs, K. W. Kolasinski, R. J. Madix and R. N. Zare, *J. Chem. Phys.*, 1987, **87**, 5038.
16 D. C. Jacobs and R. N. Zare, *J. Chem. Phys.*, submitted.
17 A. C. Kummel, G. O. Sitz and R. N. Zare, *J. Chem. Phys.*, 1988, **88**, 6707.
18 Hindered rotation of chemisorbed molecules has been directly observed. See for example, M. D. Alvey, J. T. Yates Jr and K. J. Uram, *J. Chem. Phys.*, 1987, **87**, 7221.
19 J. Segner, H. Robota, W. Vielhaber, G. Ertl, F. Frenkel, J. Häger, W. Krieger and H. Walther, *Surf. Sci.*, 1983, **131**, 273.
20 D. A. Mantell, R. R. Cavanagh and D. S. King, *J. Chem. Phys.*, 1986, **84**, 5131.
21 S. N. Dixit, D. L. Lynch and W. M. Huo, *Phys. Rev. A*, 1985, **32**, 1267.

Paper 8/03398F; *Received* 15*th August*, 1988